Eur. Phys. J. C 13, 485–495 (2000)
Digital Object Identifier (DOI) 10.1007/s100520000251

THE EUROPEAN PHYSICAL JOURNAL C

Improved calculations of quark distributions in hadrons: the case of the pion

B.L. Ioffe, A.G. Oganesian

Institute of Theoretical and Experimental Physics, B.Cheremushkinskaya 25, 117218, Moscow, Russia

Received: 14 July 1999 / Published online: 6 March 2000 – © Springer-Verlag 2000

Abstract. The earlier introduced method of calculation of quark distributions in hadrons, based on QCD sum rules, is improved. The imaginary part of the virtual photon forward scattering amplitude on some hadronic current is considered in the case, when initial and final virtualities of the current p_1^2, and p_2^2 are different, $p_1^2 \neq p_2^2$. The operator product expansion (OPE) in p_1^2, p_2^2 is performed. The sum rule for quark distribution is obtained using double dispersion representation of the amplitude on one side in terms of calculated in QCD OPE and on the other side in terms of physical states contributions. Double Borel transformation in p_1^2, p_2^2 is applied to the sum rule, killing background non-diagonal transition terms which deteriorated the accuracy in previous calculations. The case of the valence quark distribution in the pion is considered, which was impossible to treat by the previous method. OPE up to dimension 6 operators is performed and leading order perturbative corrections are accounted. Valence u-quark distribution in π^+ was found at intermediate x, $0.15 < x < 0.7$, and normalization point $Q^2 = 2\,\mathrm{GeV}^2$. These results may be used as input for evolution equations.

1 Introduction

The QCD sum rule approach, invented by Shifman, Vainstein and Zakharov in 1979 [1] is now well known as a powerful method, which makes it possible to calculate in QCD in a model independent way and with a good accuracy various hadron characteristics like masses, decay widths, form factors etc. The method is based on the operator product expansion (OPE), extended to the non-perturbative region. These results were obtained from consideration of 2- and 3-point correlators (for a review, see [2]). A bit later the structure functions, quark distributions in photon and hadrons were investigated in the QCD sum rule framework. The second moment of the photon structure function was considered in [3], and that of the pion and nucleon in [4,5], but unfortunately it was difficult to extend this approach for calculating higher moments. The general method for calculating hadron structure functions in the region of intermediate x was suggested in [6] and developed in [7]. The method is based on the consideration of a 4-point correlator, corresponding to forward scattering of two currents, one of which has the quantum numbers of the hadron of interest, and the other is electromagnetic (or weak). In the first order of OPE, in the case when the hadron is a meson, this corresponds to box diagrams like shown in Fig. 1 at $p_1 = p_2 = p, q_1 = q_2 = q$, where p is the momentum of the hadron current and q is the momentum of the photon. The problem of such diagrams is that even if p^2, q^2 are large and negative, in the case of forward scattering the singularity in the t-channel for massless quarks is at $t = 0$, i.e. large distances in the t-channel are of importance. However, as was shown in [6,7], the situation changes drastically when the imaginary part of the scattering amplitude – the object of interest in the case of structure functions – is considered. The imaginary part

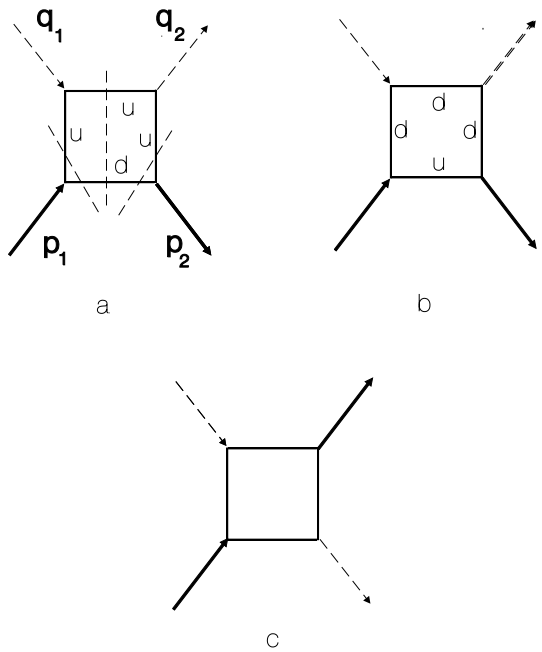

Fig. 1. Diagrams corresponding to the unit operator contribution. Dashed lines with arrows correspond to the photon, thick solid ones to the hadron current

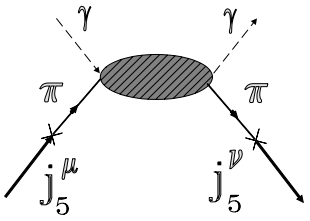

Fig. 2. Diagram of the forward photon–pion scattering

in the s-channel ($s=(q+p)^2$) of the forward scattering amplitude is dominated by small distance contributions at large (negative) p^2 and intermediate x. (Here the standard notation is used: x is the Bjorken scaling variable, $x=-q^2/2\nu$, $\nu=pq$). The proof of this statement, given in [7], is based on the fact that for the imaginary part of the forward amplitude the position closest to zero, the singularity in the momentum transfer, is determined by the boundary of the Mandelstam spectral function, and is given by the equation

$$t=-4\frac{x}{1-x}p^2. \tag{1}$$

It is assumed, that $\mid q^2 \mid \gg \mid p^2 \mid$. Therefore, for the case that the imaginary part of the forward scattering amplitude is not at small x and large p^2 the virtualities of intermediate states in the t-channel are large enough for OPE to be applicable. The further procedure is common with those for the QCD sum rules (with some special nuances we will discuss later), i.e. the dispersion representation on p^2 is saturated by physical states and the contribution of the lowest particle state is extracted using a Borel transformation. In [7] the structure function of the nucleon was calculated. Somewhat later, the structure function of the photon was also calculated [8]. But one should note that the sum rule for the d-quark distribution in the proton obtained in [7] is applicable within the rather narrow range of $(0.2<x<0.45)$ and the agreement with experiment is not good enough. Moreover, it was found to be impossible to calculate the structure functions of the π- and ρ-mesons in this way (that is why the authors of [8] were forced to use a special trick, based on VDM, to calculate the ρ-meson structure function). The reason for this is that the sum rules, in the form used in [7], have a serious drawback.

To understand what kind of problem occurs, let us briefly review the main points of the method. Consider a 4-point correlator with two electromagnetic currents and two currents with quantum numbers of some hadron (for clarity the axial current, corresponding to charged pions, will be considered but the conclusion is independent of the choice of the current). We have

$$\Pi_{\mu\nu\lambda\rho}(p_1,p_2;q_1,q_2)=-\int \mathrm{e}^{\mathrm{i}p_1x+\mathrm{i}q_1y-\mathrm{i}p_2z}\mathrm{d}^4x\mathrm{d}^4y\mathrm{d}^4z \times\langle 0\mid T\left\{j_{5\lambda}(x)j^{\mathrm{em}}_{\mu}(y)j^{\mathrm{em}}_{\nu}(0)j_{5\rho}(z)\right\}\mid 0\rangle$$

and

$$j_{5\lambda}=\bar{u}\gamma_5\gamma_\lambda d. \tag{2}$$

By considering the forward scattering amplitude in accord with [7], put $p_1=p_2$ at the very beginning. Among the various tensor structures of $\Pi_{\mu\nu\lambda\rho}$ it is convenient to consider the structure $(p_\mu p_\nu p_\lambda p_\rho/\nu)\cdot\tilde{\Pi}(p^2,q^2,x)$, and the imaginary part $\mathrm{Im}\Pi(p^2,q^2,x)$ in the s-channel related to the pion structure function $F_{2\pi}(x)$[1]. Let us write the dispersion relation representation of $\mathrm{Im}\tilde{\Pi}(p^2,q^2,x)$ in the p^2 variable. As was shown in [7] (see also [9,10]) the correct form of the dispersion representation is the double dispersion relation

$$\mathrm{Im}\tilde{\Pi}=a(x)+\int\limits_0^\infty\frac{\varphi(x,u)\mathrm{d}u}{(u-p^2)} +\int\limits_0^\infty\int\limits_0^\infty\frac{\mathrm{d}u\mathrm{d}u'\rho(u,u',x)}{(u-p^2)(u'-p^2)}. \tag{3}$$

(We restrict ourselves to lowest twist contributions, the terms of order p^2/q^2 are neglected.) In order to derive (3) it is convenient to consider first the case, when $p_1^2\neq p_2^2$ and go to the limit $p_1^2\to p_2^2=p^2$. Then the form (3) is evident. The last term in the right hand side (r.h.s.) of (3) represents the propert double dispersion contribution, the second may be considered as the subtraction term in the variables p_1^2 or p_2^2 and the first term is the subtraction term from the second. The interesting contribution for us arises from the pion poles in the two variables u and u' in the last term in (3). This term corresponds to the diagram of Fig. 2, where the axial current creates the pion; then the process of deep inelastic scattering of the virtual photon off the pion proceeds and finally the pion is absorbed by the axial current. Evidently this term is proportional to the pion structure function. All other terms in (3) may be considered as background. Let us accept a model for the hadronic spectrum in which ρ,φ can be represented by the contribution of the resonance (π-meson) and the continuum (s_0 is the continuum threshold)

$$\rho(u,u',x)=f(x)\delta(u-m_\pi^2)\delta(u'-m_\pi^2) +\rho^0(x)\theta(u-s_0)\theta(u'-s_0),$$
$$\varphi(x,u)=\varphi_1(x)\delta(u-m_\pi^2)+\varphi_2(x)\theta(u-s_0), \tag{4}$$

where $f(x)$ is proportional to the resonance (π-meson) structure function of interest,

$$f(x)\sim 2\pi F_2(x), \tag{5}$$

and $\varphi_{1,2}$ are some unknown functions, corresponding to non-diagonal transitions.

The substitution of (4) into (3) gives

$$\mathrm{Im}\tilde{\Pi}=\frac{f(x)}{(p^2-m_\pi^2)^2}+a(x) +\int\limits_{s_0}^\infty\int\limits_{s_0}^\infty\frac{\rho^0(x,u,u')\mathrm{d}u\mathrm{d}u'}{(u-p^2)(u'-p^2)}+\int\limits_{s_0}^\infty\frac{\varphi_2(x,u)}{(u-p^2)}\mathrm{d}u +\frac{\varphi_1(x,m_\pi^2)}{(p^2-m_\pi^2)}. \tag{6}$$

[1] As was mentioned in [7], the results are more reliable if the invariant amplitude at the kinematical structure with maximal dimension is used.

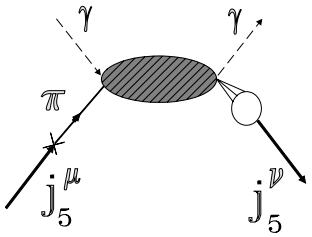

Fig. 3. Example of the non-diagonal transition

The last term in (6) corresponds to Fig. 3, where the axial current creates a pion, deep inelastic scattering proceeds, but the final state is not a pion like in Fig. 2, but some excited state with pion quantum numbers, which is absorbed by the axial current. In order to separate the term proportional to the pion structure function – the first term in the r.h.s. of (6) – the Borel transformation in p^2 is applied to (6), which suppresses continuum contributions to (6). (The Borel parameter M^2 is chosen such that $\mathrm{e}^{-s_0/M^2} \ll 1$.) After Borel transformation we get

$$\mathcal{B}_{M^2}\mathrm{Im}\tilde{\Pi}(p^2,x) = f(x)\frac{1}{M^2}\mathrm{e}^{-m_\pi^2/M^2} - \varphi_1(x)\mathrm{e}^{-m_\pi^2/M^2} + \dots \qquad (7)$$

Dots denote the terms which are suppressed exponentially after Borel transformation (the second and third terms in (6)). For these terms we can assume that they are given by the contribution of the bare loop in the same region, see Fig. 1. Because of the Borel suppression $\sim \exp(-s_0/M^2) \ll 1$ terms are small and such an approximation does not introduce an essential error in the final result. However, the second term in the r.h.s. of (7) is not exponentially suppressed in comparison with the first. The only way to kill it is to differentiate both sides of (7) (multiplied by $\exp(m_\pi^2/M^2)$) over $1/M^2$. Just this procedure was used in [6,7] to determine the nucleon structure functions. But, as is well known, the differentiation of an approximate relation may seriously deteriorate the accuracy of the results. In QCD sum rules such a procedure increases the contribution of non-perturbative corrections and continuum contributions, and the sum rules become much worse or even fail (as for the ρ-meson). For the π-meson the situation is even worse, because direct calculations show that a bare loop contribution corresponds only to non-diagonal transitions.

In this work we suggest a modified method of calculation of the hadron structure function, which is free from these problems and is completely based on QCD sum rules. We will illustrate it by the example of the π-meson structure function calculation, which usually is the most "dangerous" case.

2 The idea of the method

The idea of the method is to consider at the begining non-equal quantities $p_1^2 \neq p_2^2$ in (2) and perform all calculations for this case. Instead (3) the dispersion representation takes the form

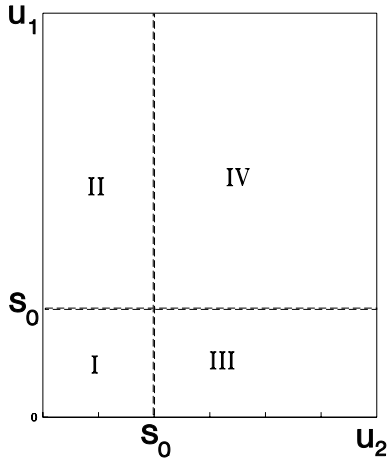

Fig. 4. Integration region in the double dispersion representation

$$\mathrm{Im}\tilde{\Pi}(p_1^2,p_2^2,x) = a(x) + \int_0^\infty \frac{\varphi(x,u)}{u-p_1^2}\mathrm{d}u + \int_0^\infty \frac{\varphi(x,u)}{u-p_2^2} + \int_0^\infty \mathrm{d}u_1 \int_0^\infty \mathrm{d}u_2 \frac{\rho(x,u_1,u_2)}{(u_1-p_1^2)(u_2-p_2^2)}. \qquad (8)$$

Apply to (8) a double Borel transformation in p_1^2, p_2^2, which kills the first three terms in the r.h.s. of (7). We then have

$$\mathcal{B}_{M_1^2}\mathcal{B}_{M_2^2}\mathrm{Im}\tilde{\Pi}(p_1^2,p_2^2,x) = \int_0^\infty \mathrm{d}u_1 \int_0^\infty \mathrm{d}u_1 \rho(x,u_1,u_2)\exp\left[-\frac{u_1}{M_1^2}-\frac{u_2}{M_2^2}\right]. \qquad (9)$$

One can divide the integration region over $u_{1,2}$ into four areas (Fig. 4):

(I) $u_1 < s_0; u_2 < s_o$;
(II) $u_1 < s_0$; $u_2 > s_0$;
(III) $u_2 < s_0$; $u_1 > s_0$;
(IV) $u_{1,2} > s_0$.

Using the standard QCD sum rule model of the hadronic spectrum and the hypothesis of quark–hadron duality, i.e. the model with one lower resonance plus continuum, one can easily notice[2] that area (I) corresponds to the resonance region. The spectral density can be written in this area as

[2] We restrict ourselves to the simplest model, because a higher resonance contribution in any case will be suppressed after double borelization.

$$\rho(u_1,u_2,x)=f_\pi^2\cdot 2\pi F_2(x)\delta(u_1-m_\pi^2)\delta(u_2-m_\pi^2), \quad (10)$$

where f_π is defined as

$$\langle 0\mid j_{\lambda 5}\mid \pi\rangle = f_\pi p_\lambda \quad f_\pi = 131\,\mathrm{MeV}.$$

In the area (IV), where both variables $u_{1,2}$ are far from the resonance region, the non-perturbative effects may be neglected, and, as usual in sum rules, the spectral function of the hadron state is described by the bare loop spectral function ρ^0 in the same region,

$$\rho(u_1,u_2,x)=\rho^0(u_1,u_2,x). \quad (11)$$

In the areas (II) and (III) one of the variables is far from the resonance region, but the other is in the resonance region, and the spectral function in this region is some unknown function $\rho=\psi(u_1,u_2,x)$, which corresponds to transitions like the $\pi\to$ continuum, as shown in Fig. 3. After double Borel transformation the total answer for the physical part can be written as (M_1^2, M_2^2 are the Borel masses squared)

$$\begin{aligned}\hat B_1\hat B_2[\mathrm{Im}\Pi] &= 2\pi F_2(x)\cdot f_\pi^2 \mathrm{e}^{-m_\pi^2\left(1/M_1^2+1/M_2^2\right)}\\ &+\int_0^{s_0}\mathrm{d}u_1\int_{s_0}^{\infty}\mathrm{d}u_2\psi(u_1,u_2,x)\mathrm{e}^{-\left(u_1/M_1^2+u_2/M_2^2\right)}\\ &+\int_{s_0}^{\infty}\mathrm{d}u_1\int_0^{s_0}\mathrm{d}u_2\psi(u_1,u_2,x)\mathrm{e}^{-\left(u_1/M_1^2+u_2/M_2^2\right)}\\ &+\int_{s_0}^{\infty}\int_{s_0}^{\infty}\mathrm{d}u_1\mathrm{d}u_2\rho^0(u_1,u_2,x)\mathrm{e}^{-\left(u_1/M_1^2+u_2/M_2^2\right)}. \quad (12)\end{aligned}$$

In what follows we put for simplicity $M_1^2=M_2^2\equiv 2M^2$. One of the advantages of this method is that after double Borel transformation the unknown contribution of the areas (II) and (III) (the second and third terms in (12)) are exponentially suppressed. Using duality arguments we estimate the contribution of the whole non-resonance region (i.e. areas II, III and IV) to be the contribution of the bare loop in the same region and demand the value to be small (less than 30%). So, equating a physical and a QCD representation of $\tilde\Pi$, and taking in account the cancellation of the appropriate parts in the left and right sides one can write the following sum rules (we omit all term, which are suppressed after Borel transformation):

$$\mathrm{Im}\Pi^0_{\mathrm{QCD}}+\text{Power correction}=2\pi F_2(x)f_\pi^2,$$

$$\mathrm{Im}\Pi^0_{\mathrm{QCD}}=\int_0^{s_0}\int_0^{s_0}\rho^0(u_1,u_2,x)\mathrm{e}^{-(u_1+u_2)/(2M^2)}. \quad (13)$$

(The pion mass is neglected.) It can be shown (see Appendix) that for box diagram $\psi(u_1,u_2,x)\sim\delta(u_1-u_2)$, and as a consequence the second and third terms in (12) are zero in our model of the hadronic spectrum.

3 Calculation of box diagram

The diagrams, corresponding to the unit operator contribution, are shown in Fig. 1a,b. Note that the crossing diagram, shown in Fig. 1c, does not contribute, their contribution being found to be 0 in leading twist. (This is a consequence of the kinematics, so such crossing diagrams also are zero for higher dimension corrections in the leading twist.)

It is enough for us to calculate the distribution of valence u-quarks in the pion, since $\bar d(x)=u(x)$. For this reason we restrict ourselves to the calculation of $\mathrm{Im}\tilde\Pi$ for the diagram Fig. 1a.

Consider first the case $p_1=p_2$ and let us demonstrate, as was announced in Sect. 2, that in this case the box diagram contributs only to non-diagonal transitions, like in Fig. 3 and refers to background terms in (7). Diagram Fig. 1a has a contribution equal to

$$\begin{aligned}\mathrm{Im}\Pi_{\mu\nu\lambda\sigma} &= -\frac{3}{(2\pi)^2}\\ &\times\frac{1}{2}\int\frac{\mathrm{d}^4k}{k^4}\delta[(k+q)^2]\delta[(p-k)^2]\\ &\times\mathrm{Tr}[\gamma_\lambda\hat k\gamma_\mu(\hat k+\hat q)\gamma_\nu\hat k\gamma_\sigma(\hat k-\hat p)]. \quad (14)\end{aligned}$$

Calculate the trace and omit the terms, which cannot contribute to the structure $\sim p_\mu p_\nu p_\lambda p_\sigma/\nu$ of interest to us. We get

$$\begin{aligned}\mathrm{Im}\Pi_{\mu\nu\lambda\sigma} &= -\frac{12}{\pi^2}\int\frac{\mathrm{d}^4k}{k^4}k_\mu k_\nu k_\lambda(k_\sigma-p_\sigma)\\ &\times\delta[(k+q)^2]\delta[(p-k)^2]. \quad (15)\end{aligned}$$

Calculation of the integral leads to

$$\mathrm{Im}\Pi_{\mu\nu\lambda\sigma}=-\frac{3}{\pi}p_\mu p_\nu p_\lambda p_\sigma\frac{1}{\nu p^2}x^2(1-x) \quad (16)$$

(only the terms $\sim p_\mu p_\nu p_\lambda p_\sigma$ are kept) and

$$\mathrm{Im}\tilde\Pi(p^2,x)=-\frac{3}{\pi}\frac{1}{p^2}x^2(1-x). \quad (17)$$

Substitute (17) into (6) and perform a Borel transformation. We get

$$\begin{aligned}\frac{3}{\pi}x^2(1-x)(1-\mathrm{e}^{-s_0/M^2}) &= 2\pi f_\pi^2 x u_\pi(x)\frac{1}{M^2}\\ &+\varphi_1(x), \quad (18)\end{aligned}$$

where $u_\pi(x)$ is the distribution of the valence u-quarks in the pion (the pion mass is neglected). Observing the M^2 dependence in (18) it becomes evident, that in this approach the attempt to separate the pion contribution from the background by studying the M^2 dependence (e.g. differentiation over $1/M^2$) is useless – up to a small correction $\sim\mathrm{e}^{-s_0/M^2}$ the box diagram contributes to the background only.

Consider now the more promising approach $p_1^2\neq p_2^2$. Since non-equality of p_1^2, p_2^2 is important for us only for

the Borel transformation, i.e. in the denominators of the dispersion representation (8), in the calculation of the numerator, resulting in the kinematical structure $p_\mu p_\nu p_\lambda p_\alpha$ we can put $p_1 = p_2 = p$. Therefore, in order to understand the essential features of the corresponding integrals in case of non-equal p_1^2, p_2^2, it is sufficient to study instead of (14) a more simple integral,

$$\mathrm{Im}T(p_1^2, p_2^2, q^2, \nu) = \int \mathrm{d}^4k \frac{1}{k^2} \frac{1}{(k+p_2-p_1)^2} \times \delta[(k+q)^2]\delta[(p_1-k)^2]. \quad (19)$$

The direct calculation of the integral in the r.h.s. of (19) (see Appendix) shows that it may be represented in the form

$$\mathrm{Im}T(p_1^2, p_2^2, q^2, \nu) = \frac{\pi}{4\nu x} \int\limits_0^{2\nu/x} \frac{1}{u-p_1^2} \frac{1}{u-p_2^2} \mathrm{d}u. \quad (20)$$

(Higher order terms in p_1^2/q^2, p_2^2/q^2 are neglected.) At $p_1^2 = p^2$ it gives

$$\mathrm{Im}T(p^2, q^2, \nu) = \frac{\pi}{4\nu x p^2}, \quad (21)$$

as it should. Equation (20) may be rewritten in the form of the double dispersion representation (8) with $a(x) = \varphi(x) = 0$ and $\rho(u, u', x)$ proportional to $\delta(u-u')$

$$\nu \mathrm{Im}T(p_1^2, p_2^2, x) = -\frac{\pi}{4x} \int\limits_0^\infty \frac{\delta(u-u')}{(u-p_1^2)(u'-p_2^2)} \mathrm{d}u\mathrm{d}u'. \quad (22)$$

(Higher twist terms are omitted.) From this consideration it becomes clear that in order to go from the case of $p_1^2 = p_2^2 = p^2$ in the calculation of the box diagram Fig. 1a (14) to $p_1^2 \neq p_2^2$, it is enough to substitute in the final result the factor $1/p^2$ by[3]

$$\frac{1}{p^2} \to -\int\limits_0^\infty \mathrm{d}u \int\limits_0^\infty \mathrm{d}u' \frac{\delta(u-u')}{(u-p_1^2)(u'-p_2^2)}. \quad (23)$$

Therefore, instead of (17) we get

$$\tilde{\Pi}(p_1^2, p_2^2, x) = \frac{3}{\pi} x^2(1-x) \times \int\limits_0^\infty \mathrm{d}u \int\limits_0^\infty \mathrm{d}u' \frac{\delta(u-u')}{(u-p_1^2)(u'-p_2^2)}. \quad (24)$$

Perform the double Borel transformation in p_1^2, p_2^2. It kills non-desirable (depending on one variable) subtraction terms in (8) and we have the sum rule for the valence u-quark distribution in the pion,

$$u_\pi(x) = \frac{3}{2\pi^2} \frac{M^2}{f_\pi^2} x(1-x)(1-\mathrm{e}^{-s_0/M^2}), \quad (25)$$

where we put $M_1^2 = M_2^2 = 2M^2$. (As is known [11] the charactiristic values of the Borel parameters M_1^2, M_2^2 in the double Borel transformation are about twice the Borel parameters in the ordinary Borel transformation used in mass calculations.)

Before going to a more accurate consideration taking account of higher dimension operators and leading order (LO) perturbative corrections, let us discuss in more detail the unit operator contribution in order to estimate if it is reasonable. The calculation of the pion decay constant f_π, performed in [1], in the same approximation results in

$$f_\pi^2 = \frac{1}{4\pi^2} M^2(1-\mathrm{e}^{-s_0/M^2}). \quad (26)$$

Substitution of (26) into (25) gives

$$u_\pi(x) = 6x(1-x). \quad (27)$$

One may note that

$$\int\limits_0^1 u_\pi(x)\mathrm{d}x = 1, \quad (28)$$

in agreement with the fact, that in the quark-parton model there is one valence quark in the pion. Also, it can easily be verified that

$$\int\limits_0^1 x u_\pi(x)\mathrm{d}x = 1/2, \quad (29)$$

which corresponds to the naive quark model, where no sea quarks exist. So one can say that formally the unit operator contribution corresponds to the naive parton model.

Of course, (28) only formally makes sense because, as was discussed in the Introduction, our approach is correct only in some intermediate region of x. The boundaries of x, where this approach is correct, will be found if one takes into account non-perturbative power corrections. In the next section we will discuss them. At the end of this section let us discuss perturbative corrections. We take into account only LO terms, proportional to $\ln(Q^2/M^2)$, and choose $Q^2 = Q_0^2 \simeq 2\,\mathrm{GeV}^2$ for the point where we calculate our sum rules. Finally, the result for a bare loop has the form (the second term in square brackets corresponds to the perturbative correction taken into account)

$$u_\pi(x) = \frac{3M^2x}{2\pi^2 f_\pi^2}(1-x) \times \left[1 + \frac{\alpha_\mathrm{s}(\mu^2)\ln(Q^2/\mu^2)}{3\pi} \times \left(1/x + 4\ln(1-x) - \frac{2(1-2x)\ln x}{1-x}\right)\right] \times (1-\mathrm{e}^{-s_0/M^2}). \quad (30)$$

In the calculation we choose the normalization point $M^2 = \mu^2$. The fact that we take into account the α_s correction at the point $Q^2 = 2\,\mathrm{GeV}^2$ means that our final result for the structure function (we write it in the next section) can be used as an input for the evolution, starting from this value of Q_0^2.

[3] It must be mentioned that such a substitution is valid only for the box diagram; it does not take place for more complicated diagrams considered in the next section.

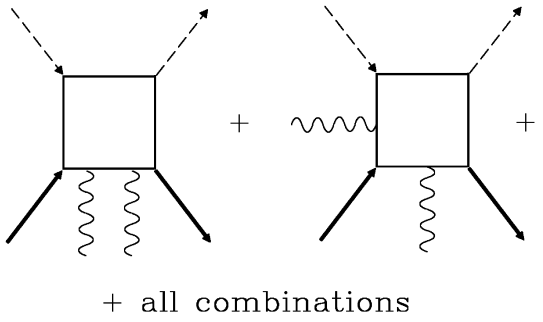

Fig. 5. Diagrams corresponding to the $d = 4$ operator contribution. Dashed lines with arrows correspond to the photon, thick solid ones to the hadron current, wave lines correspond to the external gluon field

4 Calculations of higher order terms in OPE

In this section we discuss the power correction contribution to the sum rules. The power correction with lower dimension is proportional to the gluon condensate $\langle G^q_{\mu\nu} G^q_{\mu\nu}\rangle$ with $d = 4$. As was discussed above, only s-channel diagrams (Fig. 1a) exist in the case of double borelization. The $\langle G^q_{\mu\nu} G^q_{\mu\nu}\rangle$ correction was calculated in a standard way in the Fock–Schwinger gauge $x_\mu A_\mu = 0$ [12].

The quark propagator $iS(x, y) = \langle\psi(x)\bar\psi(y)\rangle$ in the external field A_μ has the well-known form [13] (our sign of g is opposite to that of [13])

$$\begin{aligned} \mathrm{i}S(x,y) &= \mathrm{i}S^0(x-y) \\ &\quad - g\int \mathrm{d}^4 z \mathrm{i}S^0(x-z)\cdot \mathrm{i}\hat A(z)\mathrm{i}S^0(z-y) \\ &\quad + g^2\int\int \mathrm{d}^4 z\mathrm{d}^4 z' \mathrm{i}S^0(x-z)\mathrm{i}\hat A(z) \\ &\quad \times \mathrm{i}S^0(z-z')\cdot \mathrm{i}\hat A(z')\cdot \mathrm{i}S^0(z'-z) + \ldots \quad (31) \end{aligned}$$

Here S^0 is a free quark propagator; $\hat A = (1/2)\lambda^a \gamma_\mu A^a_\mu$ and

$$\begin{aligned} A^a_\mu(x) &= \left(\frac{1}{2}\right) x_\rho G^a_{\rho\mu} + \left(\frac{1}{3}\right) x_\alpha x_\rho [D_\alpha G^a_{\rho\mu}(0)] \\ &\quad + \left(\frac{1}{8}\right) x_\alpha x_\rho x_\beta [D_\alpha D_\beta G^a_{\rho\mu}]. \quad (32) \end{aligned}$$

When calculating one should take into account the quark propagator expansion up to the third term and only the first term in the expansion of the external field A_μ (Fig. 5).

These diagrams have been calculated using a program for analytical calculations, REDUCE. Surprisingly, in the case of the double borelization the sum of all diagrams in Fig. 5 was found to be 0. So the gluon condensate contribution to the sum rule is absent.

Before we discuss the $d = 6$ contribution, let us make the following remark. Due to the fact that we are interested only in the intermediate values of x, we should take into account only loop diagrams. Really one can easily see that the diagrams with no loops (like those in Fig. 6) are proportional to $\delta(1 - x)$ which is out of the region of applicability of the method.

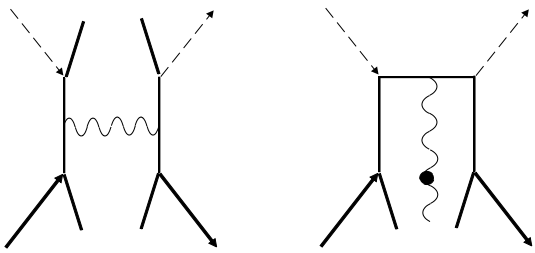

Fig. 6. Examples of the non-loop diagrams of dimension 4. Wave lines corespond to gluons, a dot means a derivative, other notations as in Fig. 1

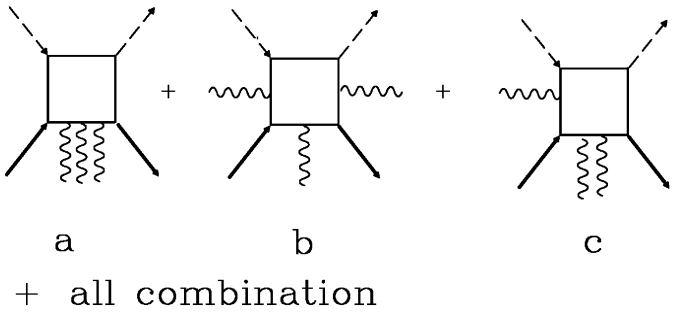

Fig. 7. Diagrams of dimension 6, see text. All notations are as in Fig. 6

There is a large number of loop diagrams corresponding to $d = 6$ corrections. First of all, there are diagrams which correspond to interaction with only the gluon vacuum field, i.e. only with external soft gluon lines (see Fig. 7). Such diagrams may appear, if we take

(1) all possible combinations which appear when the expansion of the quark propagator (31) is taken into account up to the fourth term and in the expansion of the external gluon field (32) only the first term is kept. For example, it is the fourth term of the expansion for one quark propagator and the first term (free propagator) for the other three (Fig. 6a), or the second term of the expansion for the three quark propagator and one propagator is free (Fig. 6b) etc.;
(2) all possible combinations, when the second and the third terms of the expansion of gluon field (32) are taken into account, like those shown in Fig. 7c. An external gluon line with dot corresponds to derivatives of the gluon lines.

The diagrams of Fig. 7a,b are, obviously, proportional to $\langle g^3 f^{abc} G^a_{\mu\nu} G^b_{\alpha\beta} G^c_{\rho\sigma}\rangle$ and when calculating it is convenient to use the representation of this tensor structure suggested in [14]

$$\begin{aligned} &\langle 0 \mid g^3 f^{abc} G^a_{\mu\nu} G^b_{\alpha\beta} G^c_{\rho\sigma} \mid 0\rangle \quad (33) \\ &= 1/24\langle 0 \mid f^{abc} G^a_{\gamma\delta} G^b_{\delta\epsilon} G^c_{\epsilon\gamma} \mid 0\rangle \\ &\times (g_{\mu\sigma} g_{\alpha\nu} g_{\beta\rho} + g_{\mu\beta} g_{\alpha\rho} g_{\sigma\nu} + g_{\alpha\sigma} g_{\mu\rho} g_{\nu\beta} + g_{\rho\nu} g_{\mu\alpha} g_{\beta\sigma} \\ &- g_{\mu\beta} g_{\alpha\sigma} g_{\rho\nu} - g_{\mu\sigma} g_{\nu\beta} g_{\alpha\rho} - g_{\alpha\nu} g_{\mu\rho} g_{\beta\sigma} - g_{\beta\rho} g_{\mu\alpha} g_{\nu\sigma}). \end{aligned}$$

The diagrams of Fig. 7c are proportional to $\langle 0 \mid D_\rho G^a_{\mu\nu} D_\tau G^a_{\alpha\beta} \mid 0\rangle$ and $\langle 0 \mid G^a_{\mu\nu} D_\rho D_\tau G^a_{\alpha\beta} \mid 0\rangle$. Using the equation of motion it was found in [14] that

$$
\begin{aligned}
&-\langle 0 \mid D_\rho G^a_{\mu\nu} D_\sigma G^a_{\alpha\beta} \mid 0\rangle = \langle 0 \mid G^a_{\mu\nu} D_\rho D_\sigma G^a_{\alpha\beta} \mid 0\rangle \\
&= 2O^- \left[g_{\rho\sigma}(g_{\mu\beta}g_{\alpha\nu} - g_{\mu\alpha}g_{\nu\beta})\right. \\
&+ \frac{1}{2}\left.(g_{\mu\beta}g_{\alpha\sigma}g_{\rho\nu} + g_{\alpha\nu}g_{\mu\rho}g_{\beta\sigma} - g_{\alpha\sigma}g_{\mu\rho}g_{\nu\beta} - g_{\rho\nu}g_{\mu\alpha}g_{\beta\sigma})\right] \\
&+ O^+(g_{\mu\sigma}g_{\alpha\nu}g_{\beta\rho} + g_{\mu\beta}g_{\alpha\rho}g_{\sigma\nu} - g_{\mu\sigma}g_{\alpha\rho}g_{\nu\beta} - g_{\rho\beta}g_{\mu\alpha}g_{\nu\sigma}),
\end{aligned}
$$

$$
\begin{aligned}
O^\pm &= \frac{1}{72}\langle 0 \mid g^2 j^a_\mu j^a_\mu \mid 0\rangle \\
&\pm \frac{1}{48}\langle 0 \mid g f^{abc} G^a_{\mu\nu} G^b_{\nu\lambda} G^c_{\lambda\mu} \mid 0\rangle, \qquad (34)
\end{aligned}
$$

where $j^a_\mu = \sum\limits_i \bar\psi_i \gamma_\mu (\lambda^a/2)\psi_i$.

From (34) and (34) one may note that these tensor structures are proportional to two different vacuum averages:

$$\langle 0 \mid g^2 j^2_\mu \mid 0\rangle \text{ and } \langle 0 \mid g^3 G^a_{\mu\nu} G^b_{\nu\rho} G^c_{\rho\mu} f^{abc} \mid 0\rangle.$$

The first of these, $\langle 0 \mid g^2 j^2_\mu \mid 0\rangle$, by use of the factorization hypothesis easily reduces to $\langle g\bar\psi\psi\rangle^2$ which is well known,

$$\langle 0 \mid g^2 j^2_\mu \mid 0\rangle = -(4/3)[\langle 0 \mid g\bar\psi\psi \mid 0\rangle]^2. \qquad (35)$$

But $\langle 0 \mid g^3 G^a_{\mu\nu} G^b_{\nu\rho} G^c_{\rho\mu} f^{abc} \mid 0\rangle$ is not well known; there are only some estimates based on the instanton model [15, 16]. Fortunately, in the sum of all diagrams of these two types, all terms proportional to this dimension 6 gluonic condensate are exactly cancelled and the sum of the diagrams of Fig. 7 is proportional only to $\langle g\bar\psi\psi\rangle^2$.

We consider now another type of diagrams which also give a contribution to the $d = 6$ power corrections. Such diagrams appear when one should take into consideration the expansion of the quark field:

$$
\begin{aligned}
\psi(x) &= \psi(0) + x_{\alpha_1}[\nabla_{\alpha_1}\psi(0)] \\
&+ \frac{1}{2} x_{\alpha_1} x_{\alpha_2}[\nabla_{\alpha_1}\bar\nabla_{\alpha_2}\psi(0)] + \ldots, \qquad (36)
\end{aligned}
$$

where ∇ is the covariant derivative.

In this case there appear diagrams like those in Figs. 8–10, where a quark (and antiquark) line is expanded, and the first and the second terms of the expansion (36) are taken. The expansion of the external gluon field (32) is also accounted up to the second term. For the diagrams of Fig. 10 the gluon propagator in the external field is also accounted (we discuss this below).

All these diagrams can be divided into two types with quite a different physical meaning. The first type of diagrams – like those in Fig. 8 – corresponds to the case where all interactions with the vacuum proceed out of the loop. Such diagrams correspond to logarithmic corrections (evolution) to the corresponding non-loop diagrams (without a hard gluon line). Since, as was discussed in Sect. 3, we will not take into account these non-loop diagrams, it seems reasonable that at the same level of accuracy we do not take into account their evolution. So, all the diagrams of this type should be omitted. The problem of correctly calculating non-loop diagrams and their leading logarithmic correction is a special problem, which will not be discussed here. In any case, estimates and physical arguments show that their contribution would be significant at large x and negligible in the intermediate region. We will see at the end of this paper that sum rules themselves indicate the region of x where effects of the non-loop diagrams and their evolution may be neglected.

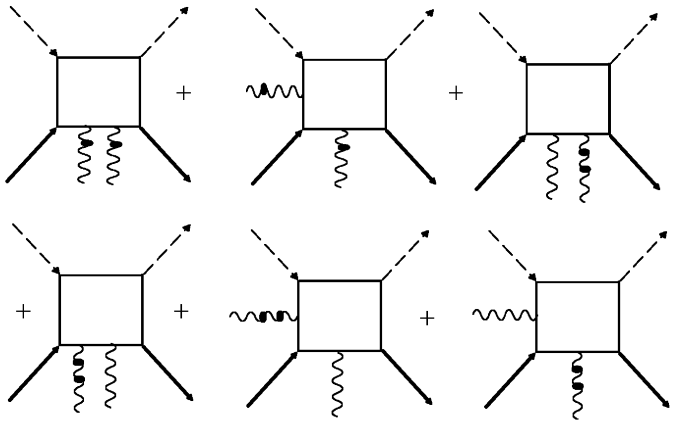

Fig. 8. Diagrams of dimension 6. External lines with dots correspond to derivatives in external fields. All notations are as in Fig. 6

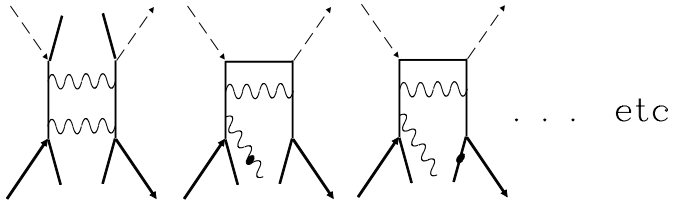

Fig. 9. Dimension 6 diagrams without the loop vacuum interaction. All notations are as in Fig. 8

So, according to the previous discussion, we should bear in mind only those diagrams where the interaction with the vacuum takes place inside the loop (Figs. 9 and 10). Such diagrams cannot be treated as the evolution of any non-loop diagrams and are pure power corrections of dimension 6. All these diagrams are, obviously, proportional to

$$\langle 0 \mid \bar\psi^d_\alpha \psi^b_\beta D_\rho G^n_{\mu\nu} \mid 0\rangle, \quad \langle 0 \mid \bar\psi^d_\alpha (\nabla_\tau \psi^b_\beta) G^n_{\mu\nu} \mid 0\rangle,$$
$$\langle 0 \mid (\nabla_\tau \bar\psi^d_\alpha)\psi^b_\beta G^n_{\mu\nu} \mid 0\rangle.$$

These tensor structures were considered in [9] where using the equation of motion the following results were obtained:

$$
\begin{aligned}
&\langle 0 \mid \bar\psi^d_\alpha \psi^b_\beta (D_\sigma G_{\mu\nu})^n \mid 0\rangle = \frac{g\langle 0 \mid \bar\psi\psi \mid 0\rangle^2}{3^3 \cdot 2^5} \\
&\times (g_{\sigma\nu}\gamma^\mu - g^{\sigma\mu}\gamma_\nu)_{\beta\alpha}(\lambda^n)^{bd}, \\
&\langle 0 \mid \bar\psi^d_\alpha (\nabla_\sigma \psi_\beta)^b G^n_{\mu\nu} \mid 0\rangle = \frac{g\langle 0 \mid \bar\psi\psi \mid 0\rangle^2}{3^3 \cdot 2^6} \\
&\times [g^{\sigma\mu}\gamma_\nu - g^{\sigma\nu}\gamma_\mu - \mathrm{i}\varepsilon^{\sigma\mu\nu\lambda}\gamma^5\gamma_\lambda]_{\beta\alpha}(\lambda^n)^{bd}. \qquad (37)
\end{aligned}
$$

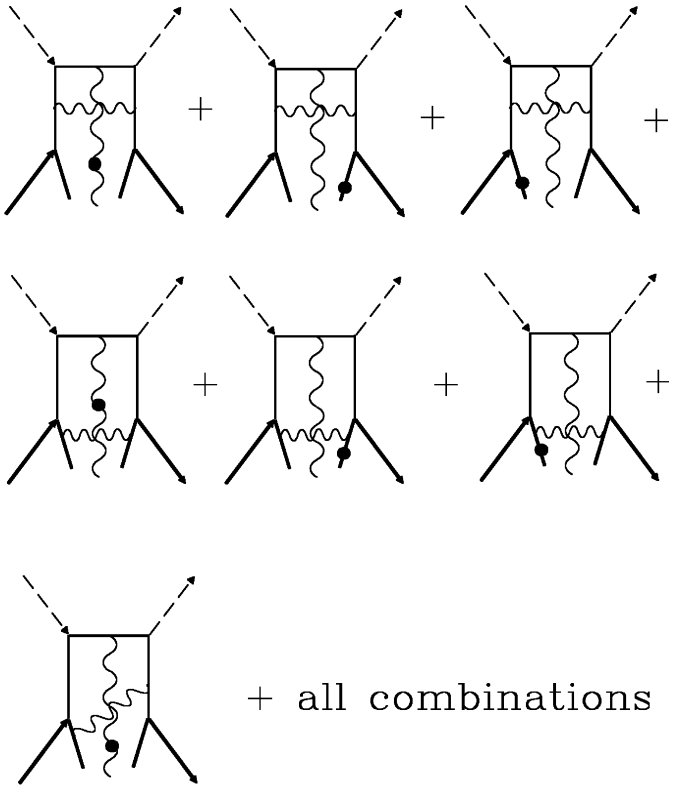

Fig. 10. Diagrams of dimension 6, corresponding to the quark propagator expansion (37). All notations are as in Fig. 8

The term $\langle 0 \mid (\nabla_\sigma \bar\psi_\alpha)^d \bar\psi^b_\beta G^n_{\mu\nu} \mid 0\rangle$ can easily be calculated using the results of [9]:

$$\langle 0 \mid (\nabla_\sigma \bar\psi_\alpha)^d \bar\psi^b_\beta G^n_{\mu\nu} \mid 0\rangle = \frac{g\langle 0 \mid \bar\psi\psi \mid 0\rangle^2}{3^3 \cdot 2^6} \times [g^{\sigma\mu}\gamma_\nu - g^{\sigma\nu}\gamma_\mu + \mathrm{i}\varepsilon^{\sigma\mu\nu\lambda}\gamma^5\gamma_\lambda]_{\beta\alpha}(\lambda^n)^{bd}.$$

For diagrams in Fig. 10 we use the following expansion of the gluon propagator:

$$S^{np}_{\nu\rho}(x-y,y) = \frac{-\mathrm{i}}{(2\pi)^4} g f^{npl} \times \int \frac{\mathrm{d}^4k}{k^4} \mathrm{e}^{-\mathrm{i}ku} \cdot \left\{ \left[-\mathrm{i}k_\lambda y_\alpha G^l_{\alpha\lambda} - \frac{2}{3}\mathrm{i}\,(y_\alpha y_\beta k_\lambda - \frac{\mathrm{i}y_\beta}{k^2}(k^2\delta_{\alpha\lambda} - 2k_\alpha k_\lambda)\right)(D_\alpha G_{\beta\lambda})^l + \frac{1}{3}\left(y_\alpha + \frac{2\mathrm{i}k_\alpha}{k^2}\right) \times (D_\lambda G_{\alpha\lambda})^l \right] \delta_{\nu\rho} + 2\left[G^l_{\nu\rho} + 2\mathrm{i}\frac{k_\alpha}{k^2}(D_\alpha G_{\nu\rho})^b \right] \right\}. \quad (38)$$

This expression can be found using the method of the calculation of the gluon propagator in the external vacuum gluon field suggested in [12]. The same result up to a $\sim G$ term is explicitly written in [13] (see also [17]). The total number of $d = 6$ diagrams is enormous – about 500. All of them were calculated using the REDUCE program. The final result for $d = 6$ corrections after double Borel transformation has the form

$$\mathrm{Im}\Pi^{d=6} = -\frac{1}{(2\pi)^7} \cdot g^2 \cdot \frac{(ga)^2}{M^4} \cdot \frac{1}{3^6 \cdot 2^5} \times \times [(-5784x^4 - 1140x^3 - 20196x^2 + 20628x - 8292)\ln(2) + 4740x^4 + 8847x^3 + 2066x^2 - 2553x + 1416]\frac{1}{x(1-x)^2}. \quad (39)$$

$(ga)^2 \equiv 4\pi\alpha_\mathrm{s} \cdot (2\pi)^4 \langle 0 \mid \bar\psi\psi \mid 0\rangle^2$. Before we write the final result of the sum rules, let us make one remark. One can see that in the contribution of the $d = 6$ operators (39) the strong coupling constant g^2 appears as a factor, and again it appears in the structures $(ga)^2$. The factor g^2 corresponds to the interaction with the quark propagators (vertices of a hard gluon line in the diagrams in Figs. 9 and 10, or vertices of external gluon in the diagrams in Figs. 6 and 7), and it is reasonable to take it at the renormalization point $\mu^2 = Q_0^2$. On the other hand, g^2 in the structure $(ga)^2$ appears as a consequence of using the equation of motion, and its normalization point should be taken in such a way that the quantity $\alpha_\mathrm{s}\langle 0 \mid \bar\psi\psi \mid 0\rangle^2$ is a renormalization group invariant. Finally, substituting the results for the bare loop (30) and the power corrections (39), we can write the sum rule for the quark distribution function in the pion:

$$xu_\pi(x) = \frac{3}{2\pi^2}\frac{M^2}{f_\pi^2}x^2(1-x) \times \left[\left(1 + \left(\frac{\alpha_\mathrm{s}(M^2)\cdot\ln(Q_0^2/M^2)}{3\pi}\right) \times \left(\frac{1+4x\ln(1-x)}{x} - \frac{2(1-2x)\ln x}{1-x}\right)\right) \cdot \left(1 - \mathrm{e}^{-s_0/M^2}\right) - \frac{4\pi\alpha_\mathrm{s}(Q_0^2)\cdot 4\pi\alpha_\mathrm{s}(M^2)a^2}{(2\pi)^4\cdot 3^7\cdot 2^6\cdot M^6} \cdot \frac{\omega(x)}{x^3(1-x)^3} \right], \quad (40)$$

where $\omega(x)$ is the expression in square brackets in (39). We choose the effective LO QCD parameter $\Lambda_{QCD} = 200\,\mathrm{MeV}$, $Q_0^2 = 2\,\mathrm{GeV}^2$. The value of the renormalization invariant parameter is equal to

$$\alpha_\mathrm{s}a^2 = \alpha_\mathrm{s}(M^2 = 1\,\mathrm{GeV}^2)\cdot(0.55\,\mathrm{GeV}^3)^2 = 0.13\,\mathrm{GeV}^6.$$

The value of a was taken from the best fit [18] of the sum rule of the nucleon masses (see [9], Appendix B). The continuum threshold was varied in the interval $0.8 < s_0 < 1.2\,\mathrm{GeV}^2$ and it was found that the results only slightly depend on it. The analysis of the sum rule (40) shows that the requirements of self-consistency are fulfilled in the region $0.15 < x < 0.7$; the power corrections are less than 30%, and the continuum contribution is small ($< 25\%$). Stability in the Borel mass parameter M^2 dependence in the region $0.4\,\mathrm{GeV}^2 < M^2 < 0.6\,\mathrm{GeV}^2$ is good; especially in the region of $x \le 0.4$ the M^2 dependence is almost constant (see Fig. 11).

The final result for $u_\pi(x)$ (at $M^2 = 0.45\,\mathrm{GeV}^2$, $s_0 = 0.8\,\mathrm{GeV}^2$) is shown in Fig. 13 (thick solid line). Figure 13 also shows the curve of the u-quark distribution in the pion, found in [19] by using the evolution equation and the data on the Drell–Yan process. (This fit does not contradict the earlier calculation of [20]). Bearing in mind

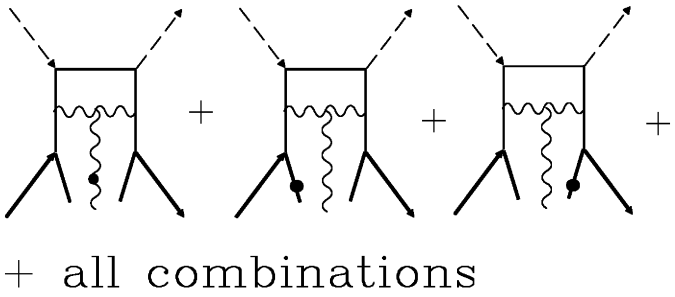

Fig. 11. Diagrams of dimension 6, corresponding to the quark and gluon propagator expansion (37) and (38). All notations are as in Fig. 8

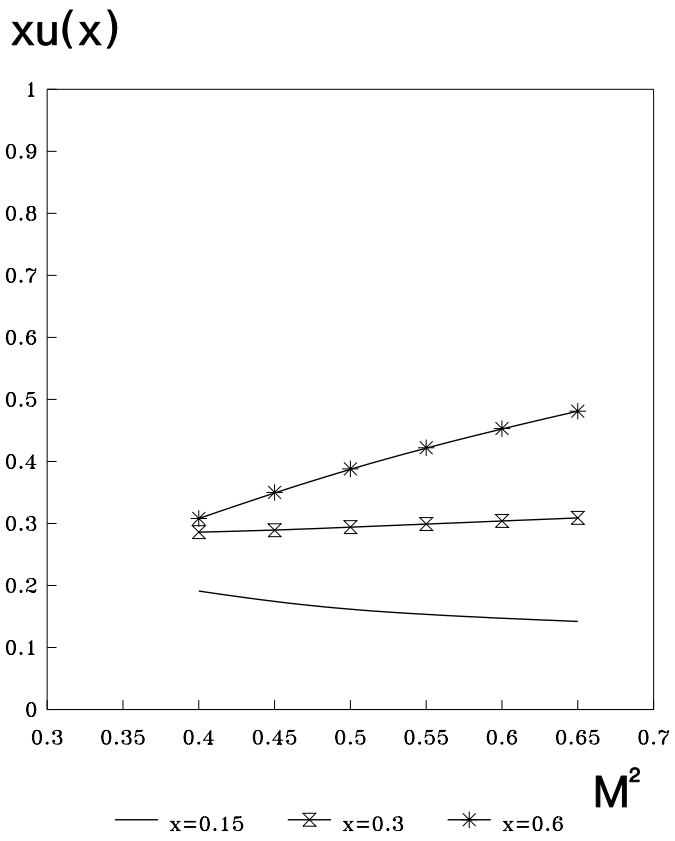

Fig. 12. Borel mass dependence of the quark distribution function at various x

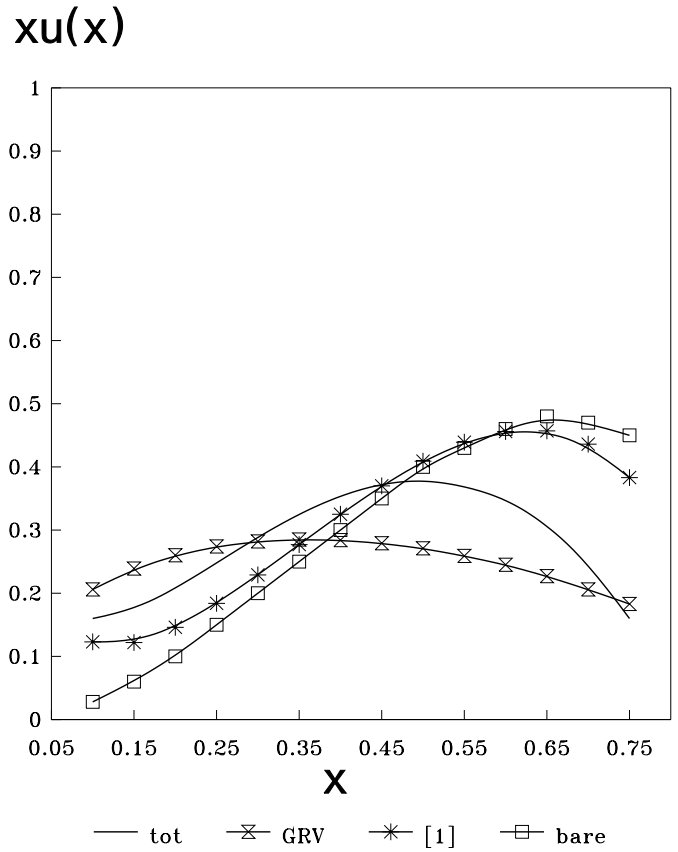

Fig. 13. Quark distribution function in pion, denoted "total". For comparison a fit from [19], denoted "GRV", is shown. Also the bare loop ("bare") and bare loop with non-perturbative corrections (denoted "1") are shown

that NLO α_s corrections are not accounted and that one may expect that they would increase $u_\pi(x)$ at low x and decrease at large x, one may consider the agreement as good. We also show in the same figure the pure bare loop contribution (line with squares) and the contribution (30) of the bare loop with non-perturbative correction (crossed line). One can see that the pure bare loop is not in quite good agreement with experiment, and both the perturbative correction and the power correction improve the agreement with experiment. Let us discuss why the stability became worse when x became larger (see Fig. 11). From our point of view, this reflects the influence of non-loop diagrams (and their evolution), which were not accounted as was discussed in Sect. 4. Indeed, the non-loop diagrams which formally are proportional to $\delta(1-x)$, really would correspond to some function with maximum close to $x=1$ and fast decreasing when x decreased. That is why effects of such diagrams (and their evolution) are negligible at $x \lesssim 0.4$–0.5, but may be more or less remarkable at large x, and the deterioration of the stability probably reflects this fact. We repeat that the obtained valence u-quark distribution function $u_\pi(x)$ can be used as input for the evolution equation (starting from the point $Q_0^2 = 2\,\mathrm{GeV}^2$).

Let us now finally discuss the estimates for the moments of the quark distribution which can be found with the help of the obtained results.

To get the moments, one should make some guesses about the region of small $x \lesssim 0.15$ and large $x \gtrsim 0.7 \div 0.8$, where our method is inapplicable. If we make the natural supposition that at $x \lesssim 0.15 u_\pi(x) \sim 1/(x)^{1/2}$ according to Regge behavior, and at large $x \gtrsim 0.7, u_\pi(x) \sim (1-x)^2$ according to the quark counting rules, then, matching these functions with our result (40), one may find that

$$\mathcal{M}_0 = \int_0^1 u_\pi(x)\mathrm{d}x \approx 0.84,$$

$$\mathcal{M}_1 = \int\limits_0^1 x u_\pi(x) \mathrm{d}x \approx 0.21$$

at $M^2 = 0.4 \div 0.45\,\mathrm{GeV}^2$. These results only slightly depend on the choice of the points of matching (not more than 5% when we vary the lower matching point in the region $0.15 \div 0.2$ and the upper one in the region $0.65 \div 0.75$). One may note that $\mathcal{M}_0$ which has the physical meaning of the number of quarks in the pion (and should be $\mathcal{M}_0 = 1$) is really close to 1 within our accuracy $\sim 10 \div 20\%$ $\mathcal{M}_1$ has the physical meaning of the part of the momentum carried by a valence quark, and the value $\mathcal{M}_1 \approx 0.21$ is in a good agreement with the well-known fact that *two* valence quarks in the pion carry about 40% of the total momentum.

Acknowledgements. This work was supported in part by RFBR grant 97-02-16131.

Appendix

In this Appendix the double dispersion representation (22) of the integral of (19) is proved. It is convenient to change variables in (19) and put $p_1 - k = k'$. Then (19) takes the form (the prime is omitted)

$$\mathrm{Im}T(p_1^2, p_2^2, q^2, \nu) = \int \mathrm{d}^4 k \frac{1}{(p_1 - k)^2} \frac{1}{(p_2 - k)^2} \times \delta[(p_1 + q - k)^2] \delta(k^2). \quad (A.1)$$

Let us assume that $q^2 = q'^2$, $t = (p_1 - p_2)^2 = 0$ and choose the Lorenz system, where 4-vector $P = (p_1 + p_2)/2$ has only the z-component equal to P_z. From

$$t = (p_1 - p_2)^2 = p_1^2 + p_2^2 + 2p_1 p_2 = 0, \quad (A.2)$$

it follows

$$P^2 = -P_z^2 = (p_1^2 + p_2^2)/2. \quad (A.3)$$

Introduce the 4-null-vector $r = p_1 - p_2$, $r^2 = 0$,

$$rP = (p_1^2 - p_2^2)/2. \quad (A.4)$$

We have

$$p_1 = P + r/2, \quad p_2 = P - r/2. \quad (A.5)$$

Use the notation

$$qP = \nu = qp_1 = qp_2. \quad (A.6)$$

Then

$$q'p_1 = q'p_2 = \nu + (p_1^2 - p_2^2)/2, \quad qr = q'r = 0. \quad (A.7)$$

We can choose the coordinate system where the 4-vector q has only time and z-components and

$$q_z = -\nu/\sqrt{-P^2}, \quad (A.8)$$
$$q_0 = \sqrt{\nu^2 - q^2 P^2}/\sqrt{-P^2} \approx \nu/\sqrt{-P^2} = -q_z.$$

The last equality corresponds to taking account of lower twist terms. From (A.4) and (A.7) for the 4-vector r with components $r = \{r_0, r_\perp, r_z\}$ it follows that

$$r_0 = \frac{1}{2}\nu \frac{p_1^2 - p_2^2}{\sqrt{-P^2}} \frac{1}{\sqrt{\nu^2 - q^2 P^2}} \approx \frac{1}{2}\frac{p_1 - p_2^2}{\sqrt{-P^2}},$$
$$r_z = \frac{1}{2}\frac{p_1^2 - p_2^2}{\sqrt{-P^2}} \approx r_0,$$
$$r_\perp^2 = -\frac{1}{4} q^2 \frac{(p_1^2 - p_2^2)^2}{\nu^2 - q^2 P^2}. \quad (A.9)$$

The components r_0 and r_z are equal in the lowest twist approximation and of order $(-P^2)^{1/2}$ if $p_1^2 \sim p_2^2$, while $r_\perp \sim (p_1^2 - p_2^2)/\nu^{1/2}$, i.e. of the next order in this approximation and it may be neglected. The argument of the first δ function in (A.1) is equal to

$$s - 2\frac{1}{\sqrt{-P^2}}\left[\nu + P^2 + \frac{1}{4}(p_1^2 - p_2^2)\right] k_z \quad (A.10)$$
$$- \left[2\sqrt{\frac{\nu^2 - q^2 P^2}{-P^2}} + \frac{1}{2}\frac{p_1^2 - p_2^2}{\sqrt{-P^2}}\right] k_0 + r_\perp k_\perp \cos\varphi = 0,$$

where φ is the azimutal angle between $p_\perp$ and $k_\perp$. The last term in (A.11) may be omitted – it is of the next order in p^2/ν: only $(r_\perp k_\perp)^2$ may appear because of integration over φ in (A.1). (This fact can be proved by direct calculation.) From the inequality

$$k_0^2 - k_z^2 \geq 0, \quad (A.11)$$

the inequality follows which defines the integration domain over k_z in the integral (A.1):

$$k_z^2 P^2 - \sqrt{-P^2}\left[\nu + P^2 + \frac{1}{4}(p_1^2 - p_2^2)\right] k_z - \frac{1}{4}P^2 \geq 0. \quad (A.12)$$

It is convenient to use the notation

$$\upsilon = 2\sqrt{-P^2} k_z. \quad (A.13)$$

The integration domain is

$$-2\nu \leq \upsilon \leq -P^2(1 - x). \quad (A.14)$$

The denominators in (A.1) are calculated by using the relations

$$(p_1 - k)^2 = p_1^2 - 2p_1 k = p_1^2 - 2Pk - rk,$$
$$(p_2 - k)^2 = p_2^2 - 2Pk + rk, \quad (A.15)$$

$$Pk = -\sqrt{-P^2} k_z,$$
$$rk \approx r_0(k_0 + k_z) = r_0\sqrt{-P^2}(1 - x)$$
$$= \frac{1}{2}(p_1^2 - p_2^2)(1 - x). \quad (A.16)$$

(In the above equalities (A.11) and (A.9) were exploited.) As a result we get (δ functions being eliminated by integration over $k_\perp^2$ and k_0):

$$\mathrm{Im}T = \frac{\pi}{4q_0\sqrt{-P^2}}$$

$$\times \int\limits_{-2\nu}^{-P^2(1-x)} \mathrm{d}\upsilon \frac{1}{p_1^2+\upsilon-(p_1^2-p_2^2)(1-x)/2} \times \frac{1}{p_2^2+\upsilon+(p_1^2-p_2^2)(1-x)/2}. \quad \text{(A.17)}$$

Changing variables

$$\upsilon = -P^2(1-x) - ux, \quad \text{(A.18)}$$

gives the final answer

$$\mathrm{Im}T = \frac{\pi}{4\nu x} \int\limits_0^\infty \frac{1}{u-p_1^2}\frac{1}{u-p_2^2}\mathrm{d}u. \quad \text{(A.19)}$$

(The upper limit of integration was put to infinity, which is legitimate in the lowest twist approximation.)

References

1. M.A. Shifman, A.I. Vainshtein, V.I. Zakharov, Nucl. Phys. B **147**, 385, 448 (1979)
2. Vacuum structure and QCD sum rules, edited by M. Shifman (North Holland, Amsterdam 1992)
3. Ya.Ya. Balitsky, Sov. J. Nucl. Phys. **37**, 576 (1983)
4. A.V. Kolesnichenko, Yad. Fiz. **39**, 1532 (1982)
5. V.M. Belyaev, B.Yu. Block, Yad. Fiz., **43**, 706 (1986); Phys. Lett. B **167**, 99 (1986)
6. B.L. Ioffe, Pisma ZhETF, **42**, 266 (1985); **43**, 316 (1986)
7. V.M. Belyaev, B.L. Ioffe, Nucl. Phys. B **310**, 548 (1988)
8. A.S. Gorsky, B.L. Ioffe, A.Yu. Khodjamirian, A. Oganesian, Z. Phys. C **44**, 523 (1989)
9. B.L. Ioffe, A.V. Smilga, Nucl. Phys. B **232**, 109 (1984)
10. B.L. Ioffe, Phys. At. Nucl. **58**, 1492 (1995)
11. B.L. Ioffe, A.V. Smilga, Nucl. Phys. B **216**, 373 (1983)
12. A.V. Smilga, Yad. Fiz. **35**, 473 (1982)
13. V.A. Novikov, M.A. Shifman, A.I. Vainshtein, V.I. Zakharov, Fortschr. Phys. **32**, 585 (1984)
14. S.N. Nikolaev, A.V. Radjushkin, Nucl. Phys. B **213**, 189 (1983)
15. V.A. Novikov, M.A. Shifman, A.I. Vainstein, V.I. Zakharov, Phys. Lett. B **86**, 347 (1979)
16. T. Schäfer, E.V. Shuryak, Rev. Mod. Phys. **70**, 323 (1998)
17. J. Govaerts, F. de Viron, D. Gusbin, J. Weyers, Nucl. Phys. B **248**, 1 (1984)
18. B.L. Ioffe, A.G. Oganesian, Phys. Rev. D **57**, R6590 (1998)
19. M. Gluck , E. Reya, A. Vogt, Z. Phys. C **53**, 651 (1992)
20. P. Aurenche et al., Phys. Lett. B **233**, 517 (1989)